Fire-Induced Radiological Integrated Assessment

Fire properties of selected materials and products in reduce oxygen conditions

Madsen, Dan; Barton, John; van Hees, Patrick; Malmborg, Vilhelm; Gren, Louise; Gudmundsson, Anders; Pagels, Joakim

2019

Document Version:
Publisher's PDF, also known as Version of record

Fire-Induced Radiological Integrated Assessment – Fire properties of selected materials and products in reduce oxygen conditions

WP-AT: T-LU-AD_FD-01 Soot Testing Campaign: Deliverables FD02

Date: 9th of December 2019

Dan Madsen, John Barton & Patrick van Hees
Division of Fire Safety Engineering, Faculty of Engineering, Lund University

&

Vilhelm Malmborg, Louise Gren, Anders Gudmundsson and Joakim Pagels
Division of Ergonomics & Aerosol Technology,
Faculty of Engineering, Lund University

LUND
UNIVERSITY

Summary

Characterization of emissions from fires in a laboratory-controlled environment are presented in this report. The project is initiated by the CERN HSE Unit and is called FIRIA, Fire-Induced Radiological Integrated Assessment. The objective of FIRIA is to enhance the knowledge of aerosols emitted from fires in order to develop dispersion models of radiologically-activated material in case of fire. Standard cone calorimeter test were done on a variety of combustible products and materials and the results are presented in the report FD03 Fire-Induced Radiological Integrated Assessment - Fire properties of selected materials and products.

In this report, a vitiated air chamber was used to test an oil and two cables at reduced oxygen concentrations that were also tested in the FD03 report. The vitiated air chamber was attached to the standard cone calorimeter and a reduction in oxygen concentration was achieved by mixing nitrogen with compressed air. This general setup has been referred to as the open controlled atmosphere cone calorimeter (CACC).

This report contains fire properties of the oil and cables at different irradiances and oxygen concentrations. The properties included are the ignition time, mass loss rate, heat release rate per unit area (HRRPUA), carbon dioxide yield, carbon monoxide yield, heat of combustion, and extinction coefficient.

The results from the reduced oxygen concentration tests were compared with the results from the FD03 report. Some observations from the comparison are:

- An increase in the ignition time when compared to tests done in the standard cone calorimeter occurred for the oil and both cables at the lowest oxygen concentration tested for each irradiance level.
- The average carbon monoxide yields remained relatively constant or increased with decreases in the oxygen concentration.
- A reduction in the oxygen concentration generally resulted in a decrease in the mass loss rate and heat release rate per unit area (HRRPUA). However, one of the cables, referred to as cable 4 (C04), did not have a reduction in the mass loss rate and HRRPUA when exposed to an irradiance of 50 kW/m^2. Cable 8 (C08) also had a higher peak mass loss rate and peak HRRPUA when tested at an oxygen concentration of 17% though the mass loss rate and HRRPUA was lower than the standard cone calorimeter result for most of the test.

The limiting oxygen concentration using nitrogen to dilute air was also estimated at an irradiance of 20 kW/m^2 for the oil and 30 kW/m^2 for the cables. The estimated limiting oxygen concentrations were:

- Oil: between 11% (no ignition) and 13% (ignition) at an irradiance of 20 kW/m^2
- Cable 4: between 12% (no ignition) and 14% (ignition) at an irradiance of 30 kW/m^2
- Cable 8: between 13% (no ignition) and 15% (ignition) at an irradiance of 30 kW/m^2

Contents

1 Introduction

The CERN HSE Unit has extended the research within the area of emissions from fires in the project FIRIA, Fire-Induced Radiological Integrated Assessment. The objective is to enhance the knowledge of aerosols emitted from fires at specific conditions. Tests have been conducted both in well-ventilated normal ambient conditions and in reduced oxygen concentrations. The results from the well-ventilated normal ambient conditions have been presented in the report FD03 Fire-Induced Radiological Integrated Assessment - Fire properties of selected materials and products. This report is focused on the effects of reduced oxygen concentration on a fire.

1.1 Justification of oxygen reduction method

Smoke filling in an enclosed environment can reduce the oxygen concentration from the normal ambient concentration of 21%[1] [1, 2]. In a compartment fire were the oxygen concentration is decreased, it would be expected that the combustion products would be the diluents. The combustion products would likely consist mostly of carbon dioxide, carbon monoxide and water vapor. Controlling the oxygen concentration with combustion products in a laboratory with the precision and accuracy needed would present too many challenges, such as maintaining a constant oxygen concentration and flow rate. Therefore, the tests conducted in this report used nitrogen to reduce the oxygen concentration of compressed air. The following provides a justification that the use of nitrogen instead of combustion gases will provide relevant results.

1.1.1 Carbon monoxide yield

Mulholland et al. [3] provides a justification for the use of nitrogen in place of combustion products to study the effect of reduced oxygen concentrations on carbon monoxide yields. They used both nitrogen and carbon dioxide to dilute air when measuring the effect of the oxygen concentration on the carbon monoxide yield of propane and methane. For the same oxygen concentration, the carbon monoxide yield was higher for air diluted with carbon dioxide than with nitrogen. However, they found that the carbon monoxide yields for propane and methane were similar at the limiting oxygen concentration whether nitrogen or carbon dioxide was used to the dilute the air.

Mulholland et al. calculated that the adiabatic flame temperature at the limiting oxygen concentration for methane and propane was nearly the same whether nitrogen or carbon dioxide was used as the diluent. Carbon dioxide has a higher thermal capacity per mole than nitrogen, which results in a higher limiting oxygen concentration when carbon dioxide is used as the diluent than when nitrogen is used.

This led Mulholland et al. to conjecture that "…the CO yield for a given fuel is primarily determined by the flame temperature for free burn conditions ($\Phi<0.3$)". Furthermore, they expressed that this implies "…the CO yield in an actual fire environment (N_2, H_2O, and CO_2 vitiating gases) near flame extinction will be similar to the nitrogen results near extinction". Brohez et al. [4] also found similar carbon monoxide yields for pyridine at the limiting oxygen concentration when using either nitrogen or carbon dioxide as a diluent.

In a fire where smoke filling causes the decrease in oxygen concentration, the temperature of the entrained smoke-air mixture into the flames can be significantly elevated over normal

[1] All concentrations are given in volume percent unless specified otherwise

ambient temperatures. This effect has not been studied. However, it could be inferred from the relative independence at the limiting oxygen concentration of the carbon monoxide yield on the diluent used that this would also be true for elevated ambient temperatures as an increased ambient air temperature has been known to lower the limiting oxygen concentration [5]. The assumption then is that the carbon monoxide yield is dependent on the adiabatic flame temperature. For very high temperatures of entrained smoke-air mixtures, this might be a more tenuous assumption as the carbon monoxide could undergo further oxidation outside of flame. This is known to happen for high smoke layer temperatures [6].

1.1.2 Smoke

There is limited research on the effect of the type diluent gases on the smoke production. Nonetheless, Brohez et al. show similar soot yields at the limiting oxygen concentration when using nitrogen or carbon dioxide as a diluent for pyridine.

1.1.3 Mass loss rate and heat release rate

Peatros and Beyler [1] report a correlation between the mass loss rate and oxygen concentration for oxygen concentrations below 21% for various fuels. The diluent gas was either combustion gasses or nitrogen and it doesn't appear that nitrogen or combustion gases cause different mass loss rates at a given oxygen concentration. The mass loss rate should be closely tied to the heat release rate so it would be expected this would true for the heat release rate as well.

1.2 Materials and products

Tested materials and products have been chosen due to being commonly used and present at CERN facilities. The materials in the products are mainly plastics except for an oil. The products can be divided into cables, plastic sheets of different thicknesses, electrical cards, insulated magnets and an oil. The cables are both multi-conductors and with a single metal core. The materials and products are presented in the report FD03 Fire-Induced Radiological Integrated Assessment - Fire properties of selected materials and products.

1.3 Experimental setup

To conduct the tests in laboratory-controlled fire conditions, the cone calorimeter [7] was used in its base design and in the oxygen-reduced tests, with a coupled vitiated air chamber [8]. An ISO-standard for these tests in vitiated conditions is not approved yet, therefore the procedure by Werrel et al. [9] was used. The aerosol measurement was done with equipment connected to the standard soot sampling connection in the cone calorimeter ventilation duct. The dilution was set-up in two stages after a pre-cyclone (nominal cut-off diameter ~5-7µm). The primary dilution (dilution factor ~30) was conducted using a porous tube diluter and ejector diluter in series. Secondary dilution was conducted using rotating disc diluters connected prior to the Aethalometer that required lower PM concentration. For the tests with the oxygen-reduced conditions, a vitiated air chamber with a standardized metallic chimney [10] (ISO 13927) was used to prevent backflow of gases and avoid flames burning in ambient air. The oxygen depletion technique in ISO 5660-1:2015 [11] for determining the heat release rate was used for standard cone calorimeter. The experimental setup is schematically presented in Figure 1.

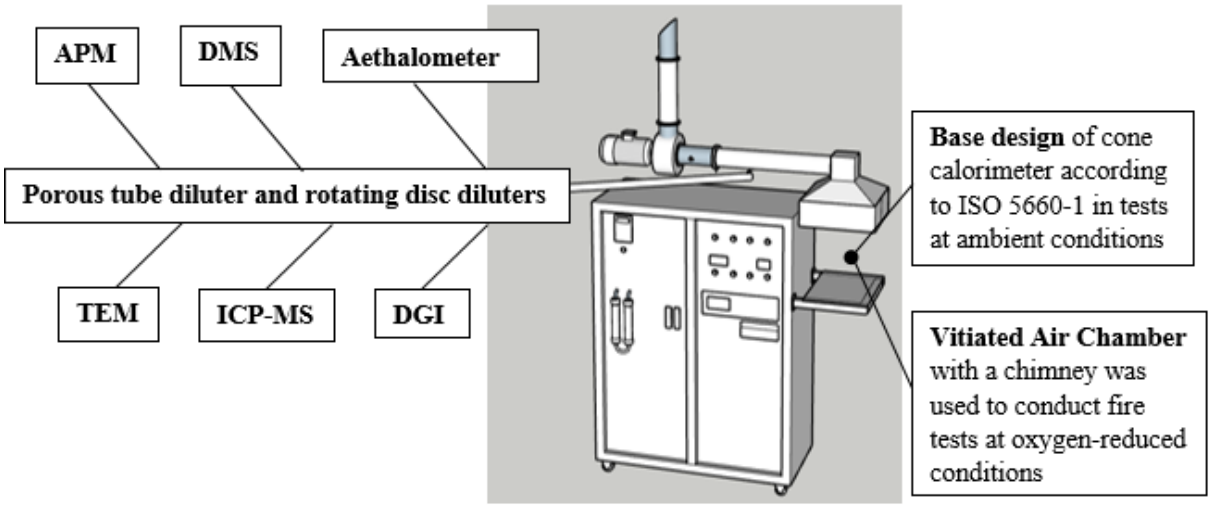

Figure 1. Schematic setup of the equipment.

A **Vitiated air chamber, VAC,** was used for oxygen reduced conditions. The chamber was fed with a continuous gas flow of controlled conditions. The flow of pressurized air and nitrogen was controlled by mass flow controllers. Two oxygen analysers were placed to show the oxygen concentration after mixing the gases as well as to measure the oxygen concentration in the vitiated air chamber. Aluminium foil was attached to the hood above the chimney to prevent exhaust gases from escaping from the hood. Figure 2 shows a photograph of the vitiated air chamber during a test and Figure 3 shows a diagram of the vitiated air chamber setup.

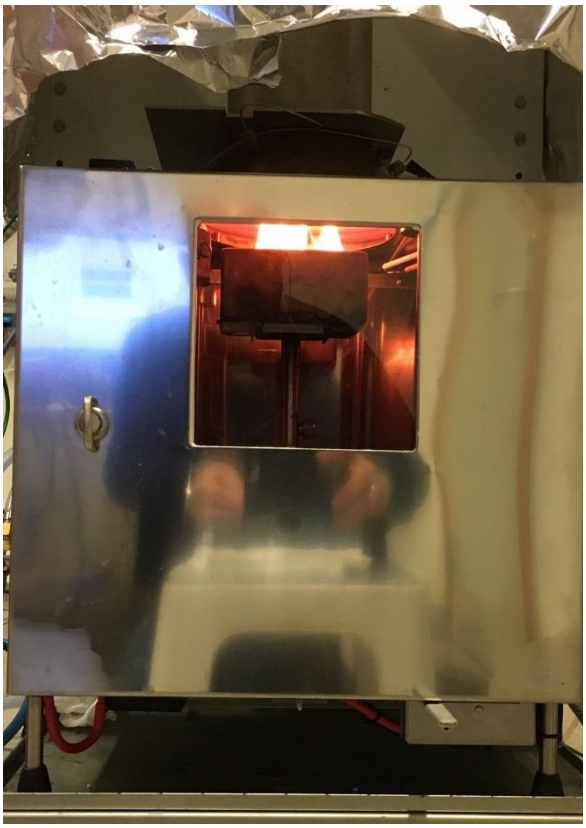

Figure 2. Vitiated air chamber during test

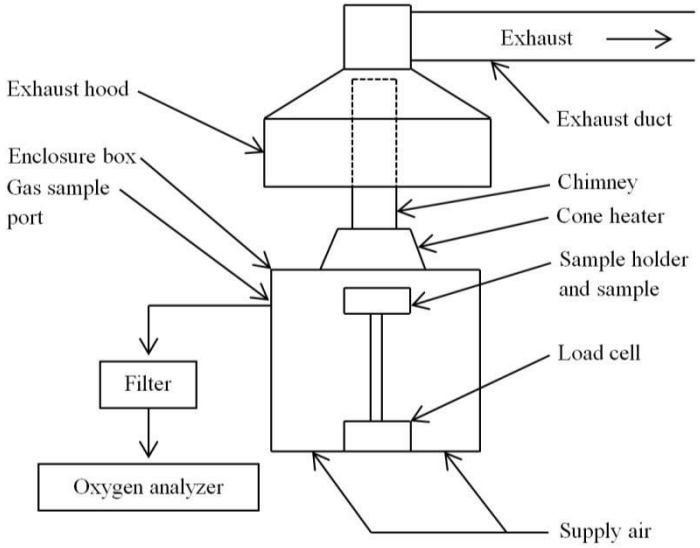

Figure 3. Diagram of the vitiated air chamber setup

Porous tube diluter and rotating disc diluters were used to arrange measurable conditions in the analysis equipment.

The **APM**, Aerosol Particle Mass analyser, was used to determine particle effective densities. A **DMA**, Differential Mobility Analyser was used prior to the APM to size-select the particles in order to measure the effective density of the selected particle sizes.

The **DMS,** Differential Mobility Spectrometer, determined the particle number size distribution.

Through the use of the **Aethalometer**, the black carbon (soot) concentration was determined by light attenuation at 7 wavelengths in the IR-VIS-UV spectrum.

With the **TEM,** Transmission Electron Microscopy, the particles were imaged so the soot structure could be analysed.

The **ICP-MS**, Inductively Coupled Plasma Mass Spectrometry**,** was used for elemental determinations.

The **DGI**, Dekati Gravimetric Impactor, sampled the aerosols in four stages to present an aerodynamic particle mass size distribution.

1.4 Method

All tested items were placed in a sample holder according to the standard procedure (ISO 5660-1:2015) in cone calorimeter tests. Cables were cut in lengths of 105 mm, products larger than the sample holder were cut with dimensions of 105x105 mm as presented in Figure 44. Cable ends were not sealed. Oils were poured in the lower part of the sample holder with an adjusted height to not hinder the movement of the igniter. The upper part of the sample holder was not used for the test of fluids. All tests were recorded with video camera for better understanding of the fire behaviour.

Figure 4. Example of cables in sample holder prior to test.

Usage of the experimental setup was coordinated by communication between operators of the cone calorimeter and of the aerosol measurement equipment. For data sampling, the cone calorimeter software, ConeCalc, was used as well as recordings for aerosol results. Test procedures varied as specific equipment was used but two general procedures are presented:

(1) Test procedure for well-ventilated normal ambient conditions. This test procedure was used for most of the tests and the experimental setup was a normal setup according to ISO 5660-1:2015 with an aerosol sampling/dilution tube connected to the soot sampling connection at the cone calorimeter ventilation duct.
(2) Test procedure for vitiated air conditions. This test procedure was used to generate conditions of reduced oxygen due to a higher content of inert gas, as nitrogen in these tests.

1.4.1 Test procedure for well-ventilated conditions

See report FD03 Fire-Induced Radiological Integrated Assessment - Fire properties of selected materials and products.

1.4.2 Test procedure, vitiated air chamber

1. Start baseline collection with enclosure door open and without flow into the enclosure.
2. Sample baseline data for 60 seconds.
3. Close the enclosure door and turn on the flow to the enclosure.
4. Wait until there is a constant O_2 concentration for the oxygen analyser connected to the enclosure and main oxygen analyser at the cone calorimeter.
5. Sample baseline data for 60 seconds.
6. Open the enclosure door, close the radiation shield, place the specimen in the enclosure, position the ignitor and close the door.
7. Wait for 70 seconds so the O_2 concentration in the enclosure can return to the specified concentration.
8. Start test by removing the radiation shield and simultaneously press the Start-button in ConeCalc. Communicate, Start test to aerosol operator.

9. End the test by closing the radiation shield.
10. Leave the specimen in the enclosure for at least 120 seconds
11. Turn off the gas sample to the enclosure.
12. Remove the specimen and place under an exhaust hood.

1.5 Calculation procedure

1.5.1 Heat release rate calculation

The methodology from Werrel et al. [9] was used to calculate the heat release rate (equations 1-4). This methodology adjusts for changes in the amount ambient air from the laboratory that is drawn into the exhaust. Werrel et al. reports that without this adjustment the heat release rate can deviate up to 30%.

$$\dot{q} = E \cdot 1.10 \cdot \left(X_{O_2}^{A^0}\gamma - X_{O_2}^{A^S}(\gamma-1)\right) \cdot C\sqrt{\frac{\Delta p}{T_e}}\left[\frac{\phi - 0.172(1-\phi)X_{CO}^A/X_{O_2}^A}{(1-\phi)+\phi\left(1+0.5\left(X_{O_2}^{A^0}\gamma - X_{O_2}^{A^S}(\gamma-1)\right)\right)}\right]\left(1 - X_{H_2O}^S\tilde{y}\right) \quad (1)$$

$$\phi = \frac{\left[\left(X_{O_2}^{A^0}\gamma - X_{O_2}^{A^S}(\gamma-1)\right)\left(1-X_{CO_2}^A - X_{CO}^A\right)\right] - \left[X_{O_2}^A\left(1-X_{CO_2}^{A^S}\tilde{y}\right)\right]}{\left(1-X_{O_2}^A - X_{CO_2}^A - X_{CO}^A\right)\left(X_{O_2}^{A^0}\gamma - X_{O_2}^{A^S}(\gamma-1)\right)} \quad (2)$$

$$\gamma = \frac{\dot{m}_e^0}{\dot{m}_e} \quad (3)$$

$$\tilde{y} = 1 - \frac{\dot{m}_g^B}{\dot{m}_e} \quad (4)$$

In this report, the HRRPUA is reported and not the heat release rate. The heat release rate was divided by an area of 0.00884 m^2 in order to calculate the HRRPUA. This area corresponds to the top opening of cone calorimeter sample holder which is exposed to the radiant heater

1.5.2 Carbon dioxide and carbon monoxide yield calculation

The following equations (5-7) from Janssens [12] for calculating the carbon dioxide and carbon monoxide mass flow rates for the standard cone calorimeter are listed below.

$$\dot{m}_{CO_2} - \dot{m}_{CO_2}^0 = \frac{X_{CO_2}^A\left(1-X_{O_2}^{A^0}\right) - X_{CO_2}^{A^0}\left(1-X_{O_2}^A - X_{CO}^A\right)}{1-X_{O_2}^A - X_{CO_2}^A - X_{CO}^A}\frac{M_{CO_2}}{M_a}\frac{\dot{m}_e}{1-\phi(\alpha-1)}\left(1 - X_{H_2O}^0\right) \quad (5)$$

$$\dot{m}_{CO} = \frac{X_{CO}^A\left(1-X_{O_2}^{A^0} - X_{CO_2}^{A^0}\right)}{1-X_{O_2}^A - X_{CO_2}^A - X_{CO}^A}\frac{M_{CO}}{M_a}\frac{\dot{m}_e}{1-\phi(\alpha-1)}\left(1 - X_{H_2O}^0\right) \quad (6)$$

$$\phi = \frac{X_{O_2}^{A^0}\left(1-X_{CO_2}^A - X_{CO}^A\right) - X_{O_2}^A\left(1-X_{CO_2}^{A^0}\right)}{\left(1-X_{O_2}^A - X_{CO_2}^A - X_{CO}^A\right)X_{O_2}^{A^0}} \quad (7)$$

These equations need to be adjusted for the open CACC for the same reason that the heat release rate equations need to be adjusted. The amount ambient air from the laboratory that is drawn into the exhaust changes during the test which affects the effective baseline values. Following the methodology of Werrel et al. for the adjustment of the of baseline concentrations in the heat release rate equation, the new carbon dioxide and carbon monoxide mass flow rates are shown below.

$$\dot{m}_{CO_2} - \dot{m}_{CO_2}^0 = \frac{X_{CO_2}^A\left(1-\left(X_{O_2}^{A^0}\gamma - X_{O_2}^{A^S}(\gamma-1)\right)\right) - X_{CO_2}^{A^S}\tilde{y}\left(1-X_{O_2}^A - X_{CO}^A\right)}{1-X_{O_2}^A - X_{CO_2}^A - X_{CO}^A}\frac{M_{CO_2}}{M_a}\frac{\dot{m}_e}{1-\phi(\alpha-1)}\left(1 - X_{H_2O}^S\tilde{y}\right) \quad (8)$$

$$\dot{m}_{CO} = \frac{X_{CO}^{A}\left(1-\left(X_{O_2}^{A^0}\gamma - X_{O_2}^{A^S}(\gamma-1)\right)-X_{CO_2}^{A^S}\tilde{y}\right)}{1-X_{O_2}^{A}-X_{CO_2}^{A}-X_{CO}^{A}}\frac{M_{CO}}{M_a}\frac{\dot{m}_e}{1-\phi(\alpha-1)}\left(1-X_{H_2O}^{S}\tilde{y}\right) \quad (9)$$

$$\phi = \frac{\left[\left(X_{O_2}^{A^0}\gamma - X_{O_2}^{A^S}(\gamma-1)\right)\left(1-X_{CO_2}^{A}-X_{CO}^{A}\right)\right]-\left[X_{O_2}^{A}\left(1-X_{CO_2}^{A^S}\tilde{y}\right)\right]}{\left(1-X_{O_2}^{A}-X_{CO_2}^{A}-X_{CO}^{A}\right)\left(X_{O_2}^{A^0}\gamma - X_{O_2}^{A^S}(\gamma-1)\right)} \quad (10)$$

$$\gamma = \frac{\dot{m}_e^0}{\dot{m}_e} \quad (11)$$

$$\tilde{y} = 1 - \frac{\dot{m}_g^B}{\dot{m}_e} \quad (12)$$

The carbon dioxide and carbon monoxide yield was then calculated by dividing the area underneath the carbon dioxide and carbon monoxide mass flow rates curves by the total mass loss during the burning period. This results in an average yield for the test.

1.5.3 Equivalence ratio

The equivalence ratio (ϕ) is the ratio of the rate of fuel burned to the rate of oxygen supplied divided by the stoichiometric ratio of fuel to oxygen [13]. This is given in equation 13.

$$\phi = \frac{\dot{m}_{fuel}/\dot{m}_{oxygen}}{\left(\dot{m}_{fuel}/\dot{m}_{oxygen}\right)_{stoichiometric}} \quad (13)$$

The equivalence ratio is normally associated with pre-mixed flames, but the concept can be extended to non-premixed flames [13]. The concept of a global equivalence ratio [6] will be used to characterize the ventilation conditions of the open CACC. The flow rate of the oxygen into the enclosure of the open CACC will be used as the mass flow rate of the oxygen in the numerator of equation 13.

The global equivalence ratio of the tests conducted in the open CACC cannot be calculated precisely because the stoichiometric ratio of the fuels is not known. Gottuk and Lattimer [6] give a method for estimating the equivalence ratio by assuming a constant energy release per mass of oxygen consumed of 13.1 MJ/kg O_2, which is shown below in equation 14.

$$\phi = \frac{\dot{Q}}{\dot{m}_a}\cdot\frac{1}{EY_{O_2,air}} \quad (14)$$

where

$\dot{Q}$ = Ideal heat release rate of the fire (kW)

$\dot{m}_a$ = Air flow rate (kg/s)

E = 13,100 kJ/kg

$Y_{O_2,air}$ = Mass concentration of oxygen

This method assumes that a complete heat of combustion is known. However, the complete heat of combustion is not known for the cables and the oil tested. Therefore, an estimated low and high heat of combustion was assumed in order to estimate the global equivalence ratio. The global equivalence ratio was calculated for the maximum mass loss rate during each test using

a low heat of combustion of 30 MJ/kg and a high heat of combustion of 55 MJ/kg. The air flow rate ($\dot{m}_a$) used was the flow rate into the enclosure of open CACC and the oxygen concentration used was the set oxygen concentration for each test. Equation 14 requires a mass concentration of oxygen so the measured volume concentration of oxygen was converted to a mass concentration.

1.5.4 Data smoothing

The mass of the test specimen was sampled every 1 s and this mass data was smoothed with a moving average over a 60 point window. The mass loss rate was then calculated using a five point numerical differential scheme from ISO 5660-1:2015 at 5 s intervals.

The time dependent heat of combustion was smoothed using a moving average over a 48 point window for 5 s intervals.

2 Results

The reduced results are introduced in this chapter. All the tests with comments are briefly presented in an Excel-sheet but an extract is presented here for each item to give an overview of measurements taken. All reports, data sampling, reduced data, photos, videos and pictures are stored electronically at https://lu.app.box.com/folder/69299876673. A table of the tested items is presented in the report FD03 Fire-Induced Radiological Integrated Assessment - Fire properties of selected materials and products.

The resulting fire properties, obtained from the cone calorimeter measurements, are presented in this chapter for each test.

As a screening test, Cable 4, C04, was tested both with sealed ends and unsealed but without any change in fire behaviour that not can be explained by usual variation in fire tests. The used sealant was a firestop sealant for building products. Nevertheless, as there were no considerable changes between the tests, all following cable tests were performed with unsealed ends.

2.1 Cable 4, C04

Cable 4 is a brown coax cable with a thermoplastic dialectric insulator and an outer diameter of 5 mm. The sales marking is DRAKA 2016 CB 50 09 3414713 6111308426187 MT. The conditions for the vitiated air tests of C04 are in Table 1.

Four tests, T53-T56-T59-T62, were performed in the vitiated air chamber. In addition, the tests at the same irradiance in the standard cone calorimeter are included in the figures. These are marked as an oxygen concentration of 21%.

Table 1. Performed tests of Cable 4, C04

Test	Irradiance [kW/m2]	Flow rate [liter/minute]	Oxygen [%]	DMS	Aethalo-meter	DGI	APM	TEM	ICP-MS	VAC
T53	50	150	17	yes	yes	no	yes	no	no	yes
T56	50	150	15	yes	yes	no	yes	no	no	yes
T59	30	120	14	yes	yes	yes	yes	yes	yes	yes
T62	30	90	12	No	No	no	No	no	no	yes

The heat release rates per unit area (HRRPUA) for the tests with an irradiance of 50 kW/m^2 are shown in Figure 5. The HRRPUA for T53 (50 kW/m^2 and 17% O_2) closely followed the HRRPUA for the tests in the standard cone calorimeter (T1 and T2). In contrast, T56 (50 kW/m^2 and 15% O_2) does not have a clear first peak in the HRRPUA. The initial HRRPUA shown for T56 is actually due to flashing before sustained ignition since the ignition time for T56 is approximately 120 s longer than for T53 and the standard cone calorimeter tests T1 and T2.

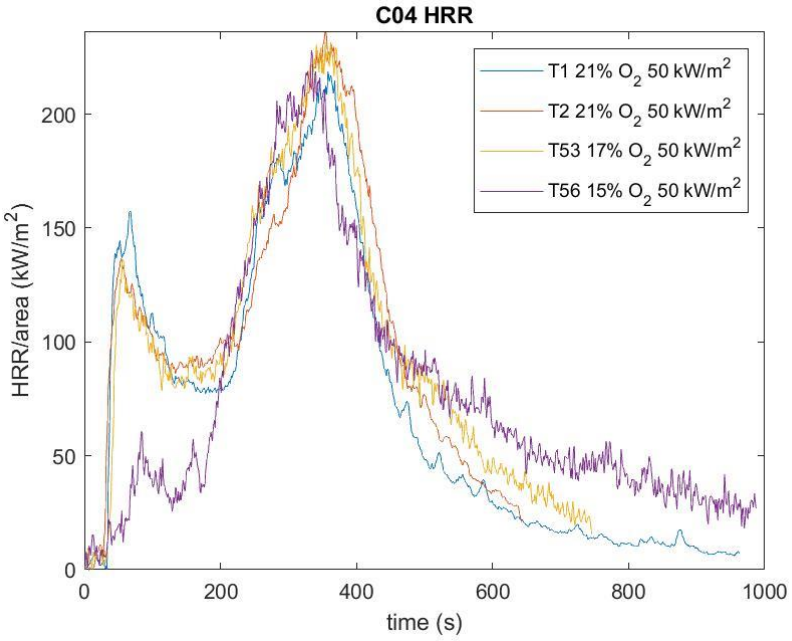

Figure 5. Heat release rates per unit area of Cable 4 at different O_2% with an irradiance of 50 kW/m^2

Figure 6 presents the HRRPUA for the tests with an irradiance of 30 kW/m^2. The HRRPUA of T59 (14% O_2) is more clearly below the HRRPUA for the standard cone calorimeter tests at the same irradiance of 30 kW/m^2 (T4 and T22). T59 also only has one distinct peak in contrast to the standard cone calorimeter tests. The low HRRPUA before ignition in T59 seems to be due to surface oxidation because an increase in the carbon monoxide concentration in the duct corresponded with a decrease in the oxygen concentration in the duct before ignition.

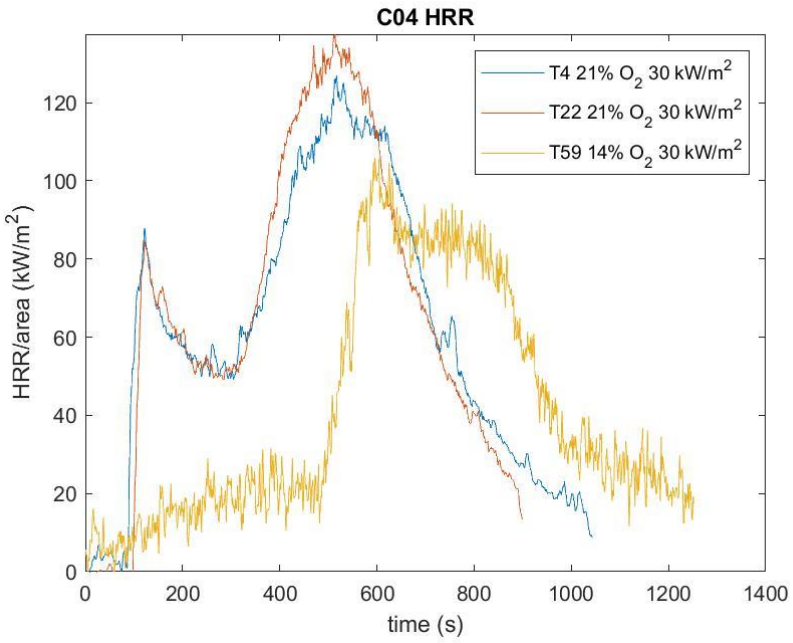

Figure 6. Heat release rates per unit area of Cable 4 at different O_2% with an irradiance of 30 kW/m^2

Figure 7 shows the mass loss rates for the tests with an irradiance of 50 kW/m^2. The mass loss rates for the low oxygen tests closely follow the mass loss rates of the tests conducted in the standard cone calorimeter. This is mostly in agreement with the HRRPUA for these tests with the exception of T56 at an oxygen concentration of 15%. The HRRPUA of T56 was much lower at the beginning of the test, which appears to be due to the longer ignition time. However, the mass loss rate was very similar at the beginning of the test. This suggests that most of the heat transfer responsible for the mass loss rate at an irradiance of 50 kW/m^2 comes from the cone heater and not the flame.

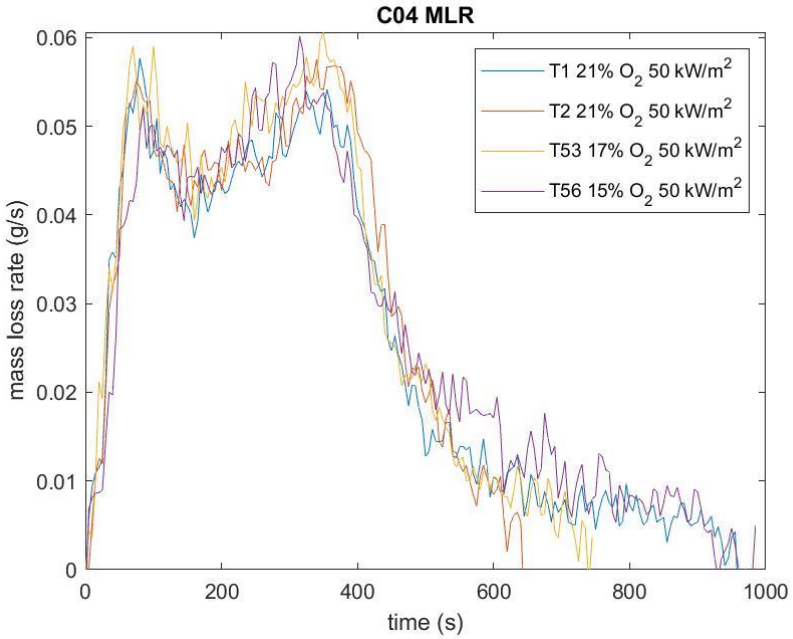

Figure 7. Mass loss rate of Cable 4 at different O_2% with an irradiance of 50 kW/m^2

Figure 8 shows the mass loss rates for the tests with an irradiance of 30 kW/m^2. The ignition time for the only test at a reduced oxygen concentration, T59, was 640 s. This makes comparing the mass loss rates more difficult because the standard cone tests were burning for a significant amount of time before reaching the ignition time of T59.

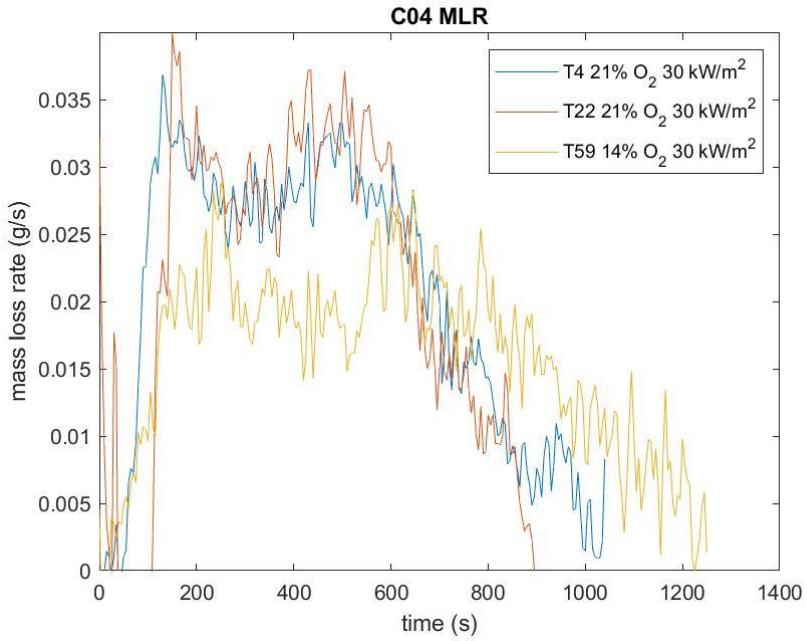

Figure 8. Mass loss rate of Cable 4 at different O_2% with an irradiance of 30 kW/m^2

Figure 9 shows the extinction coefficient for the tests with an irradiance of 50 kW/m^2. The initial peak in the extinction coefficient is before ignition so it appears that the oxygen concentration doesn't affect the extinction coefficient significantly during the burning period. The extinction coefficient doesn't account for the size of fire, but the HRRPUA were close for all of the tests.

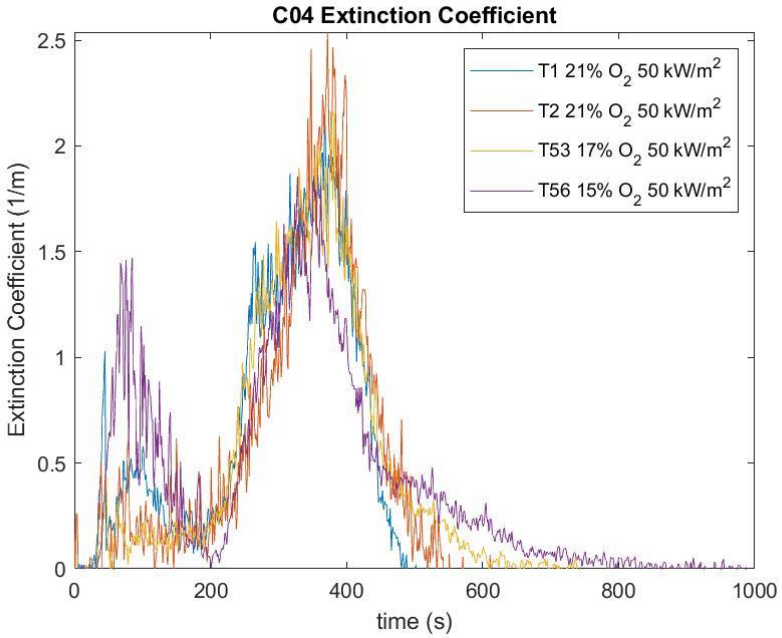

Figure 9. Extinction coefficient of Cable 4 at different O_2% with an irradiance of 50 kW/m^2

Figure 10 shows the extinction coefficient for the tests with an irradiance of 30 kW/m^2. The initial peak in the extinction coefficient for T59 is before ignition. It's hard to judge the effect of the oxygen concentration because T59 had a considerably longer ignition time. The extinction coefficient does appear to be significantly lower during the burning period for T59.

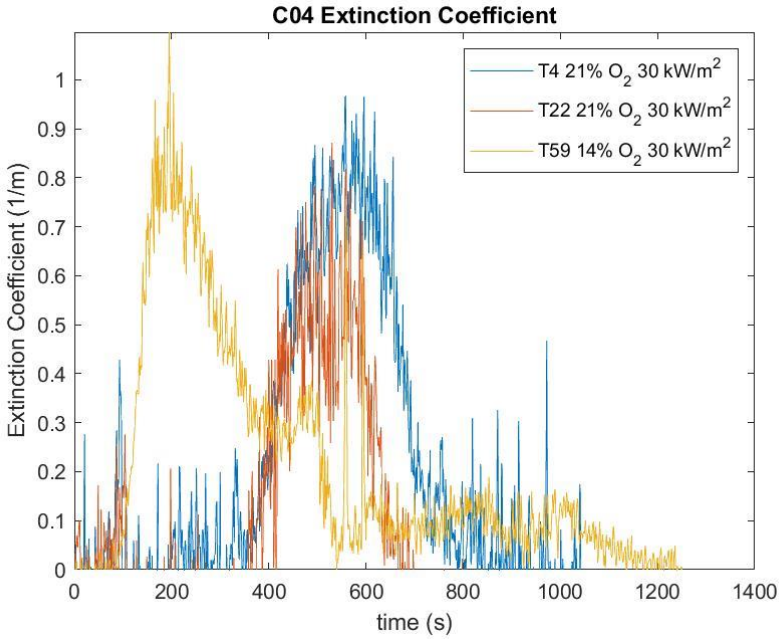

Figure 10. Extinction coefficient of Cable 4 at different O_2% with an irradiance of 30 kW/m^2

Figure 11 shows the time dependent values of the heat of combustion during each test.

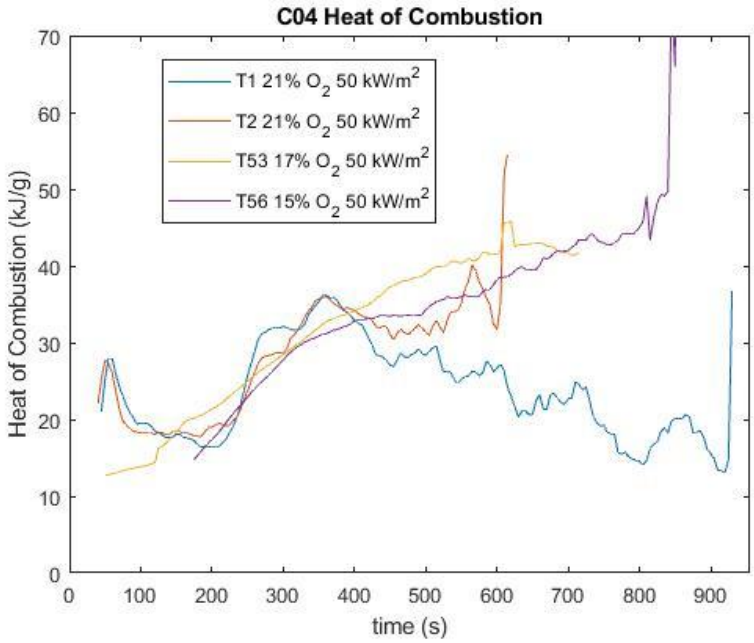

Figure 11. Heat of Combustion from ignition to 30 seconds before end of test at different O_2% with an irradiance of 50 kW/m^2

Figure 12 shows the time dependent values of the heat of combustion during each test.

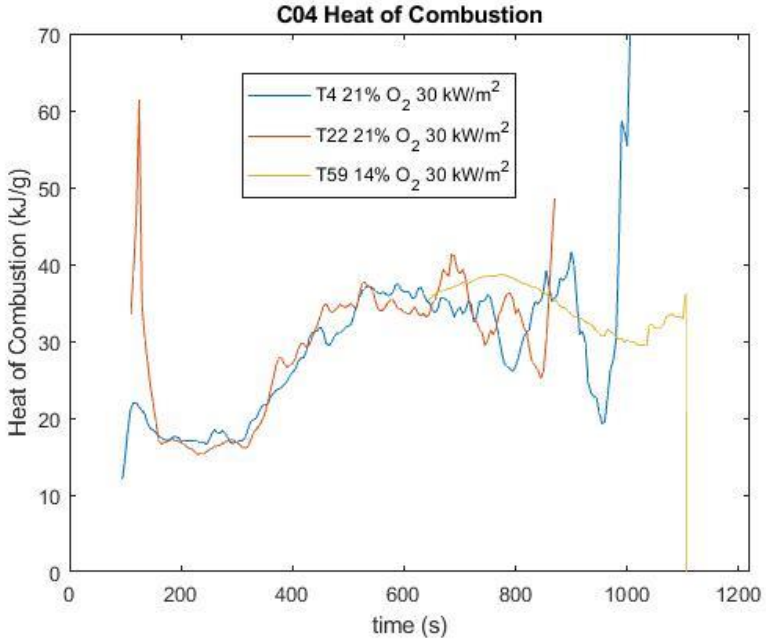

Figure 12. Heat of Combustion from ignition to 30 seconds before end of test at different O_2% with an irradiance of 30 kW/m^2

In Table 2, the resulting fire properties are presented for each test. The yields and heat of combustion are calculated as average values for the test.

Table 2. Fire properties of Cable 4 at different heat fluxes

Test	Irradiance [kW/m2]	Oxygen conc. [%]	Time to ignition [s]	CO2-yield [kg/kg]	CO-yield [kg/kg]	Heat of Combustion [MJ/kg]
T1	50	21	43	1.76	0.049	25.48
T2	50	21	39	1.87	0.036	26.80
T53	50	17	45	1.85	0.037	27.30
T56	50	15	170	1.92	0.038	31.20
T4	30	21	93	1.95	0.054	27.20
T22	30	21	105	1.99	0.035	28.71
T59	30	14	640	2.14	0.093	31.72
T62	30	12	No ignition	-	-	-

Table 3 presents the estimated global equivalence ratios. As can be seen the estimated global equivalence ratio was below 1 for all of the tests.

Table 3. Estimated global equivalence ratio

Fuel	Test ID	Irradiance (kW/m²)	O_2% vol.	$\dot{V}_{box}$ (l/min)	Max MLR (g/s)	ϕ with ΔH_c = 30 MJ/kg	ϕ With ΔH_c = 55 MJ/kg
C04	T53	50	17	150	0.060	0.24	0.40
	T56	50	15	150	0.060	0.27	0.45
	T59	30	14	120	0.030	0.18	0.30

2.2 Cable 8, C08

Cable 8 is an orange multi conductor cable with an outer diameter of 9.5 mm. The sales marking is CABLE ANTIFEU 2x1.5mm² MHF2. Five tests, T54-T57-T60-T63-T67, of Cable 8 were performed in the vitiated air chamber. The tests performed are in Table 4. In the figures, the tests at the same irradiance in the standard cone calorimeter are included. These are marked as at an oxygen concentration of 21%.

Table 4. Performed tests of Cable 8, C08.

Test	Irradiance [kW/m2]	Flow rate [liter/minute]	Oxygen [%]	DMS	Aethalo-meter	DGI	APM	TEM	ICP-MS	VAC
T54	50	150	17	yes	yes	no	yes	no	no	yes
T57	50	150	15	yes	yes	no	yes	no	no	yes
T60	30	150	17	yes	yes	yes	no	no	no	yes
T63	30	120	13	yes	yes	no	yes	no	no	yes
T67	30	150	15	yes	yes	no	no	no	no	yes

The HRRPUA for the tests with an irradiance of 50 kW/m^2 are shown in Figure 13. The HRRPUA for the tests conducted at reduced oxygen concentration T54 (17% O_2) and T57 (15% O_2), both had HRRPUA below the standard cone test T46. The maximum HRRPUA for T54 occurred at the end of the test and was higher than the peak HRRPUA for the standard cone test. The peak HRRPUA for T57 was below the standard cone test.

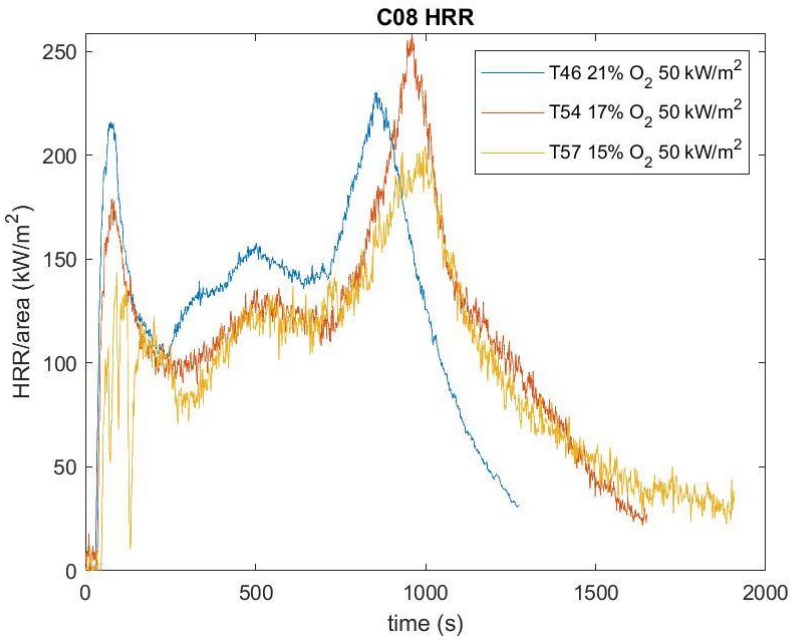

Figure 13. Heat release rates per unit area of Cable 8 at different O_2% with an irradiance of 50 kW/m^2

Figure 14 presents the HRRPUA for the tests with an irradiance of 30 kW/m^2. The HRRPUA of T60 (17% O_2) was below the standard cone calorimeter test, T11, for most of test. T67 only ignited for a short period at 1195 s. The low HRRPUA before ignition in T67 seems to be due to surface oxidation because an increase in the carbon monoxide concentration in the duct corresponded with a decrease in the oxygen concentration in the duct before ignition.

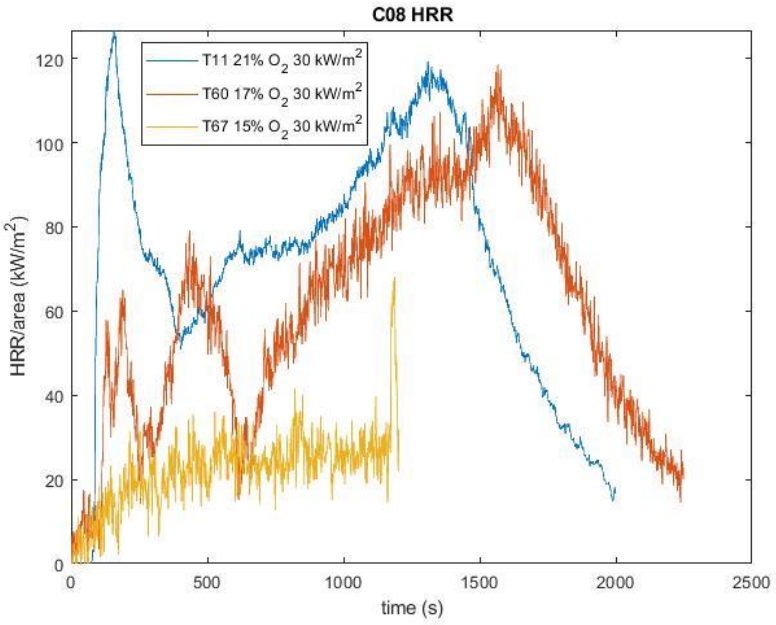

Figure 14. Heat release rates per unit area of Cable 8 at different O_2% with an irradiance of 30 kW/m^2

Figure 15 shows the mass loss rates for the tests with an irradiance of 50 kW/m^2. The mass loss rates follow a similar pattern to the HRRPUA. The reduced oxygen tests, T54 and T57,

have a mass loss rate that is below standard cone test for most of the test. The exception is the peak at the end of T54.

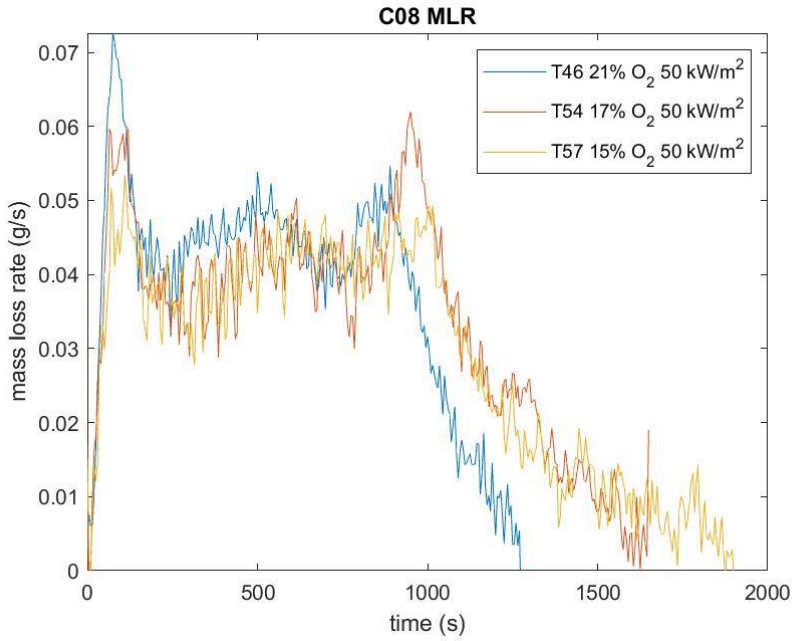

Figure 15. Mass loss rate of Cable 8 at different O_2% with an irradiance of 50 kW/m^2

Figure 16 presents the mass loss rate of the tests with an irradiance of 30 kW/m^2. There was an issue with the mass measurement of T67 and the mass loss rate was assumed to be constant for time period at the end of the test were there was issue. The problem with the mass measurement may have been caused by the ignitor pushing down on the cables due to an expansion of the cables. Nevertheless, the mass loss rates are quite similar for most of the test.

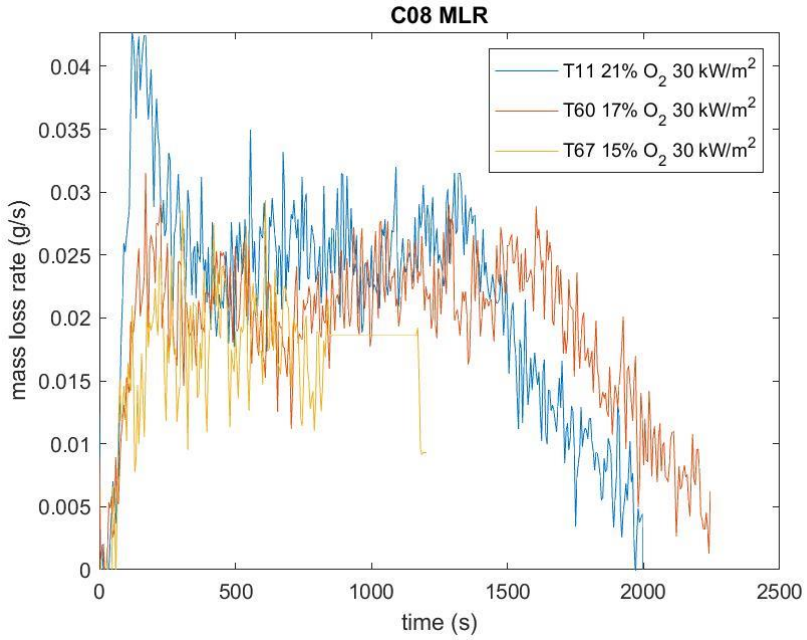

Figure 16. Mass loss rate of Cable 8 at different O_2% with an irradiance of 50 kW/m^2

The extinction coefficients are shown for an irradiance of 50 kW/m^2 in Figure 17. The reduced oxygen concentration tests were considerably below the standard cone calorimeter test.

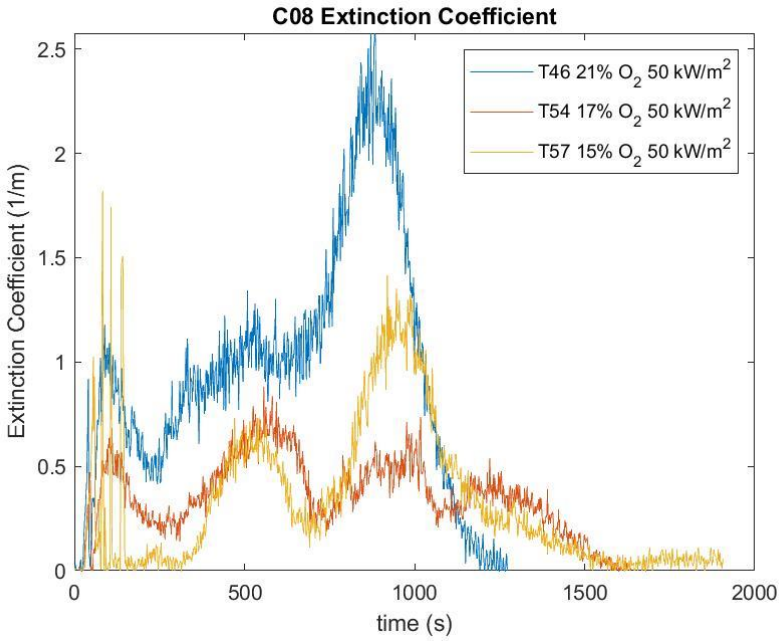

Figure 17. Extinction coefficient of Cable 8 at different O_2% with an irradiance of 50 kW/m^2

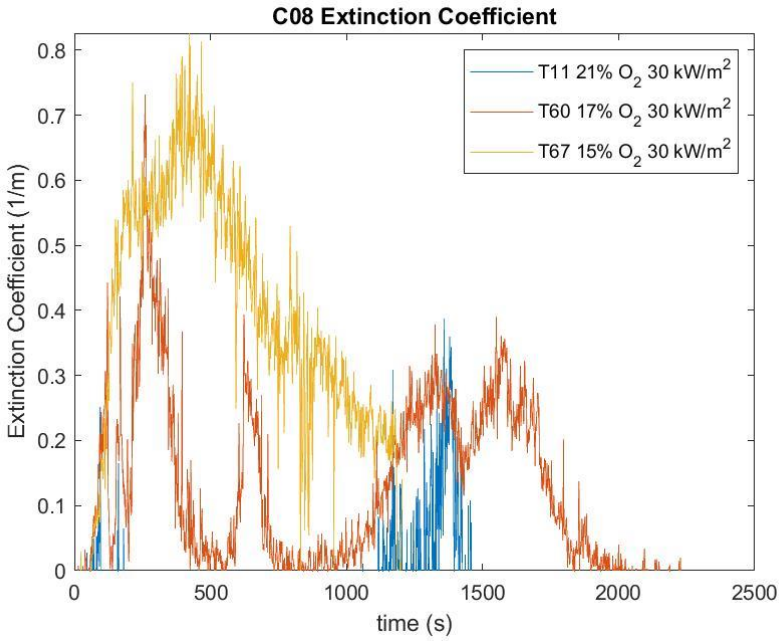

Figure 18. Extinction coefficient of Cable 8 at different O_2% with an irradiance of 30 kW/m^2

Figures 19 and 20 shows the time dependent values of heat of combustion during each test.

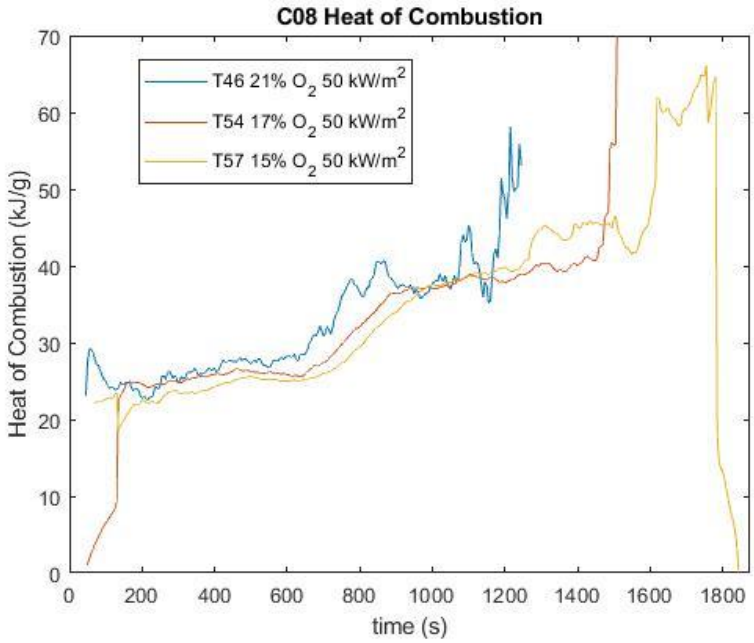

Figure 19. Heat of Combustion from ignition to 30 seconds before end of test at different O_2% with an irradiance of 50 kW/m^2

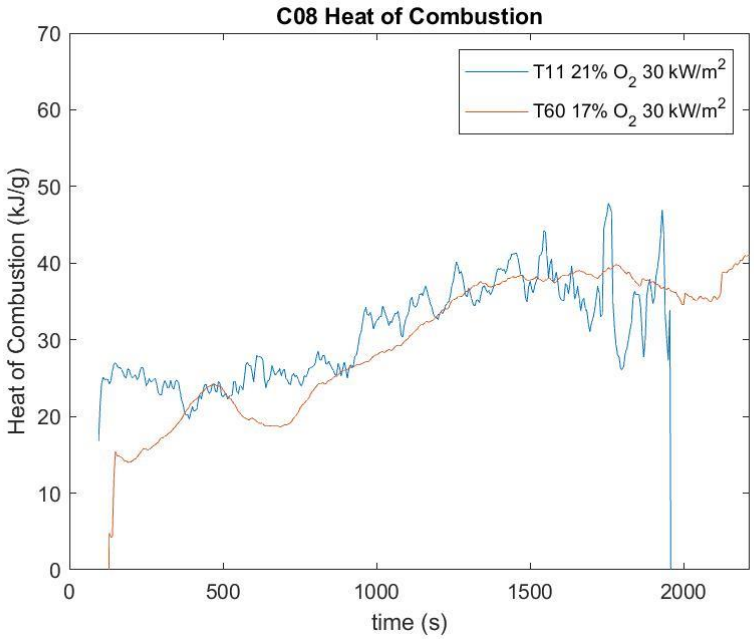

Figure 20. Heat of Combustion from ignition to 30 seconds before end of test at different O_2% with an irradiance of 30 kW/m^2

In Table 5, the resulting fire properties are presented for each test. The yields and heat of combustion are calculated as average values for the test.

Table 5. Fire properties of Cable 8 at different heat fluxes.

Test	Irradiance [kW/m2]	Oxygen conc. [%]	Time to ignition [s]	CO2-yield [kg/kg]	CO-yield [kg/kg]	Heat of Combustion [MJ/kg]
T46	50	21	40	1.93	0.027	30.08
T54	50	17	45	2.03	0.028	28.75
T57	50	15	65	1.93	0.031	30.05
T11	30	21	94	2.00	0.024	29.30
T60	30	17	123	1.82	0.061	28.97
T63	30	13	No ignition	-	-	-
T67	30	15	1195	0.70	0.098	15.19

Table 6 presents the estimated global equivalence ratios. As can be seen the estimated global equivalence ratio was below 1 for all of the tests.

Table 6. Estimated equivalence ratio

Fuel	Test ID	Irradiance (kW/m^2)	O_2% vol.	$\dot{V}_{box}$ (l/min)	Max MLR (g/s)	ϕ with ΔH_c = 30 MJ/kg	ϕ With ΔH_c = 55 MJ/kg
C08	T54	50	17	150	0.060	0.24	0.40
	T57	50	15	150	0.053	0.24	0.40
	T60	30	17	150	0.031	0.12	0.21
	T67	30	15	150	0.029	0.13	0.22

2.3 OIL, O01

Oil, O01, is an oil used in Isolde target area. The sales marking is Oil P3: D-35614 Asslar. The oil O01, was also tested twice, T58 and T61, in the vitiated air chamber with an oil depth of 5 mm, at an irradiance of 20 kW/m^2 and at different oxygen concentrations. The oil was tested in two tests as presented in Table 7. Figures 21 and 22 show photographs of the sample holder with the oil and the oil container.

Table 7. Performed tests of O01

Test	Irradiance [kW/m^2]	Flow rate [liter/minute]	Oxygen [%]	Depth [mm]	DMS	AETHALO-METER	DGI	APM	TEM	ICP-MS	VAC
T58	20	90	11	5	yes	yes	no	no	no	no	yes
T61	20	120	13	5	yes	yes	no	no	no	no	yes

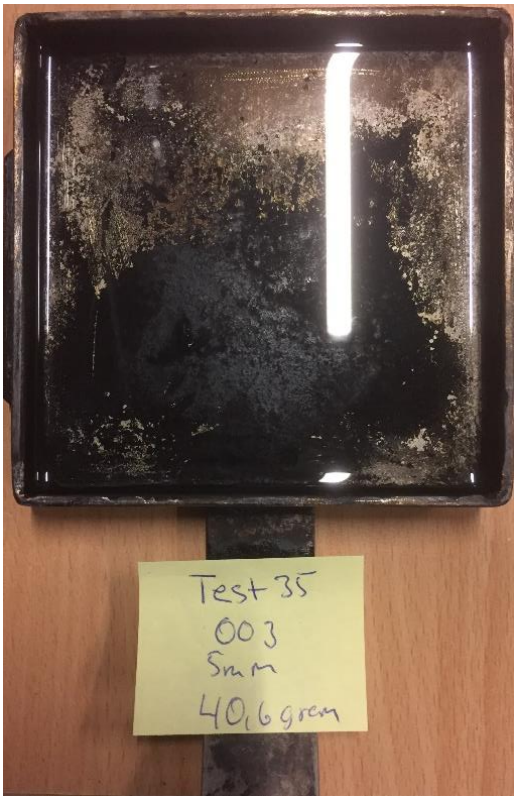

Figure 21. T35, in sample holder

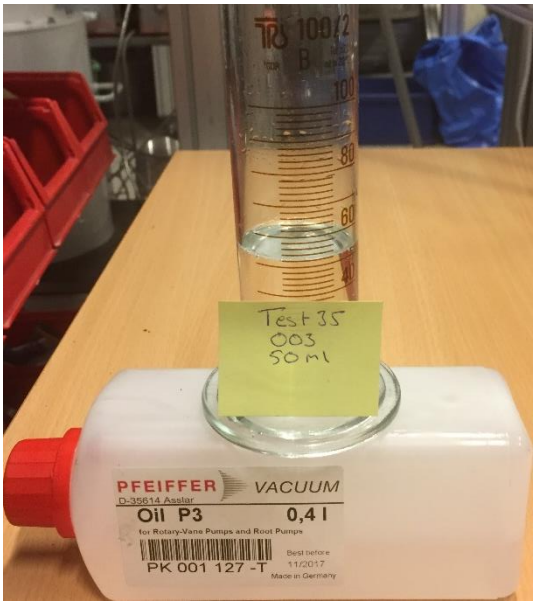

Figure 22. T35, with container

Figure 23 presents the HRRPUA of the oil. The HRRPUA for the reduced oxygen test T61 is significantly lower than the HRRPUA of the standard cone calorimeter test T37.

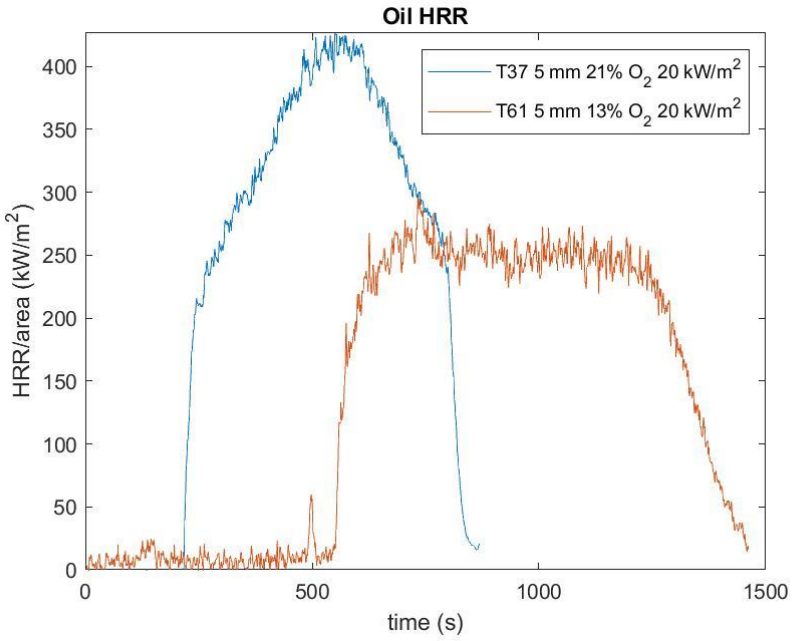

Figure 23. Heat release rates per unit area of an oil, O01, at different O_2% with an irradiance of 20 kW/m^2

Figures 24 shows the mass loss rate of the oil. The mass loss rate has a quite similar pattern to the HRRPUA.

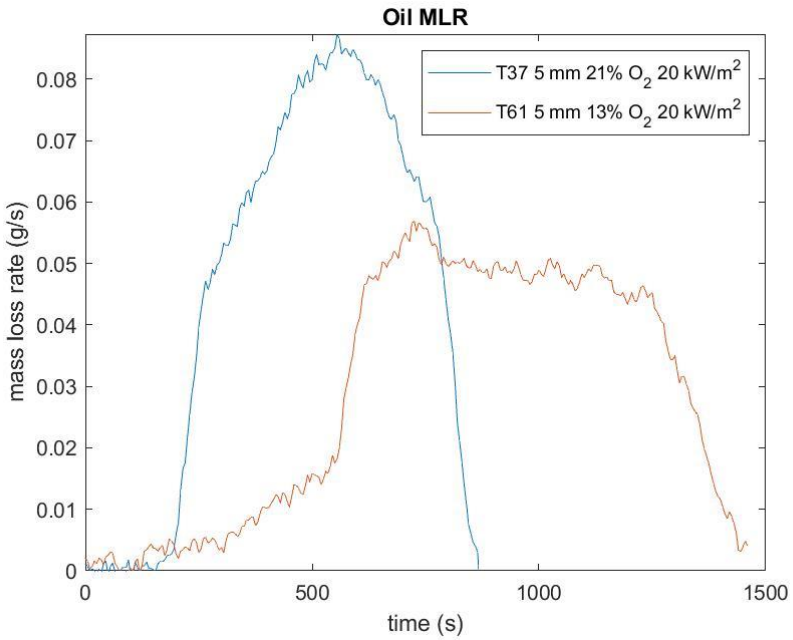

Figure 24. Mass loss rate of an oil, O01, at different O_2% with an irradiance of 20 kW/m^2

The extinction coefficient is shown in Figure 25.

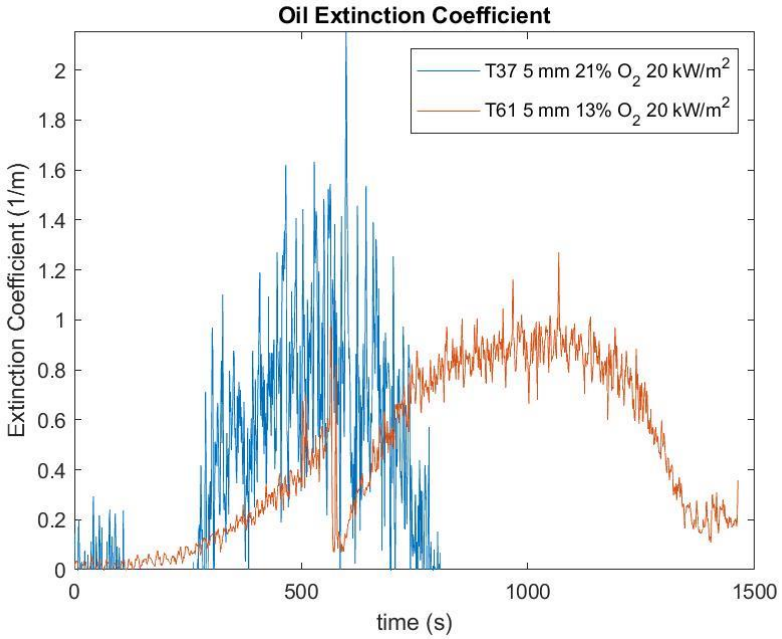

Figure 25. Extinction coefficient of oil, O01, at different O_2% with an irradiance of 20 kW/m^2

Figure 26 shows the time dependent values of heat of combustion during each test. The heat of combustion remained relatively constant for both tests.

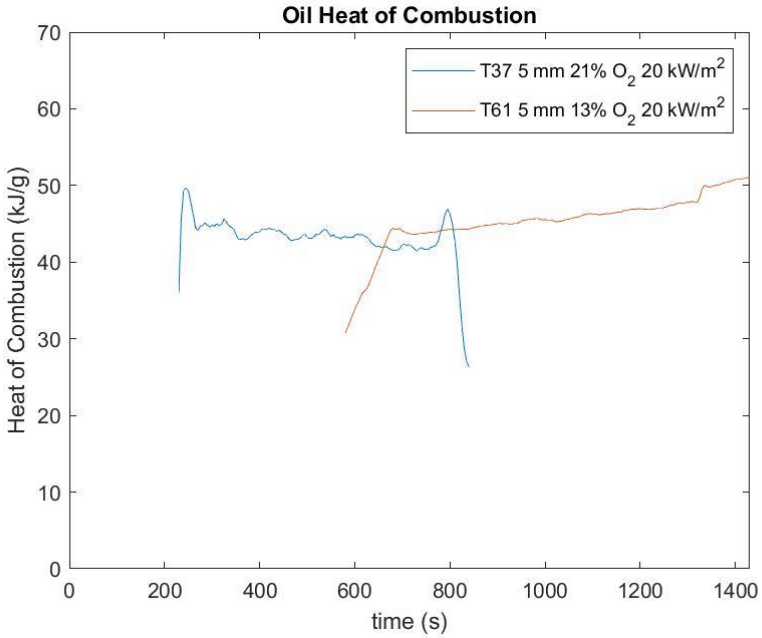

Figure 26. Heat of Combustion from ignition to 30 seconds before end of test at different O_2% with an irradiance of 20 kW/m^2

In Table 8, the resulting fire properties are presented for each test. The yields and heat of combustion are calculated as average values for the test.

Table 8. Fire properties of oil, O01, at different heat fluxes.

Test	Irradiance [kW/m2]	Oxygen conc. [%]	Time to ignition [s]	CO2-yield [kg/kg]	CO-yield [kg/kg]	Heat of Combustion [MJ/kg]
T37	20	21	226	2.59	0.041	43.04
T58	20	11	No ignition	-	-	-
T61	20	13	578	2.80	0.038	45.16

Table 9 presents the estimated global equivalence ratio for T61. As can be seen the estimated global equivalence ratio was below 1.

Table 9. Estimated equivalence ratio

Fuel	Test ID	Irradiance (kW/m^2)	O_2% vol.	$\dot{V}_{box}$ (l/min)	Max MLR (g/s)	ϕ with ΔH_c = 30 MJ/kg	ϕ With ΔH_c = 55 MJ/kg
Oil	T61	20	13	120	0.056	0.36	0.61

3 Discussion

3.1 Ignition

Ignition times have been shown to be impacted by the oxygen concentration though not under all conditions. For some fuels, there has been an increase in the ignition time when the oxygen concentration was lowered. However, the increase in ignition time was not always observed for each reduced oxygen concentration level [14].

Rich et al. [15] investigated the mass flux at ignition and flash point for black PMMA and a blended polypropylene/fiber glass in the forced ignition and flame spread test (FIST) apparatus. The mass flux at ignition increased as the oxygen concentration was reduced below 21%, but the mass flux at the flash point did not. Others have also reported an increase in mass flux at ignition when the oxygen concentration is lowered below 21% [16, 17]. The mass flux at the flash point is not reported in these studies though.

It has been proposed that the flash point occurs when the lower flammability limit of the pyrolysis gases or fuel vapors is reached at the ignitor [15, 18]. This would explain why the flash point occurs at a constant time and mass flux for different oxygen concentrations because the lower flammability limit has a low sensitivity to the oxygen concentration when a nitrogen and oxygen mixture is used [5, 15].

On the other hand, the mass flux at ignition is affected by the oxygen concentration. Unlike the mass flux at the flash point, the mass flux at ignition has to be high enough to release a sufficient amount of energy to overcome the heat losses to the fuel surface. The decrease in the oxygen concentration means there is less energy available to be lost to the fuel surface. This results in potentially higher mass fluxes at ignition and longer ignition times. The location of the ignitor plays a role though because the mass flux at the fuel surface may be high enough for ignition, but the ignitor may be far enough away from the fuel surface that the mass flux is not high enough to reach the lower flammability limit at the ignitor.

The time until the flash point and ignition for the oil, cable 4, and cable 8 is shown in Figure 27.

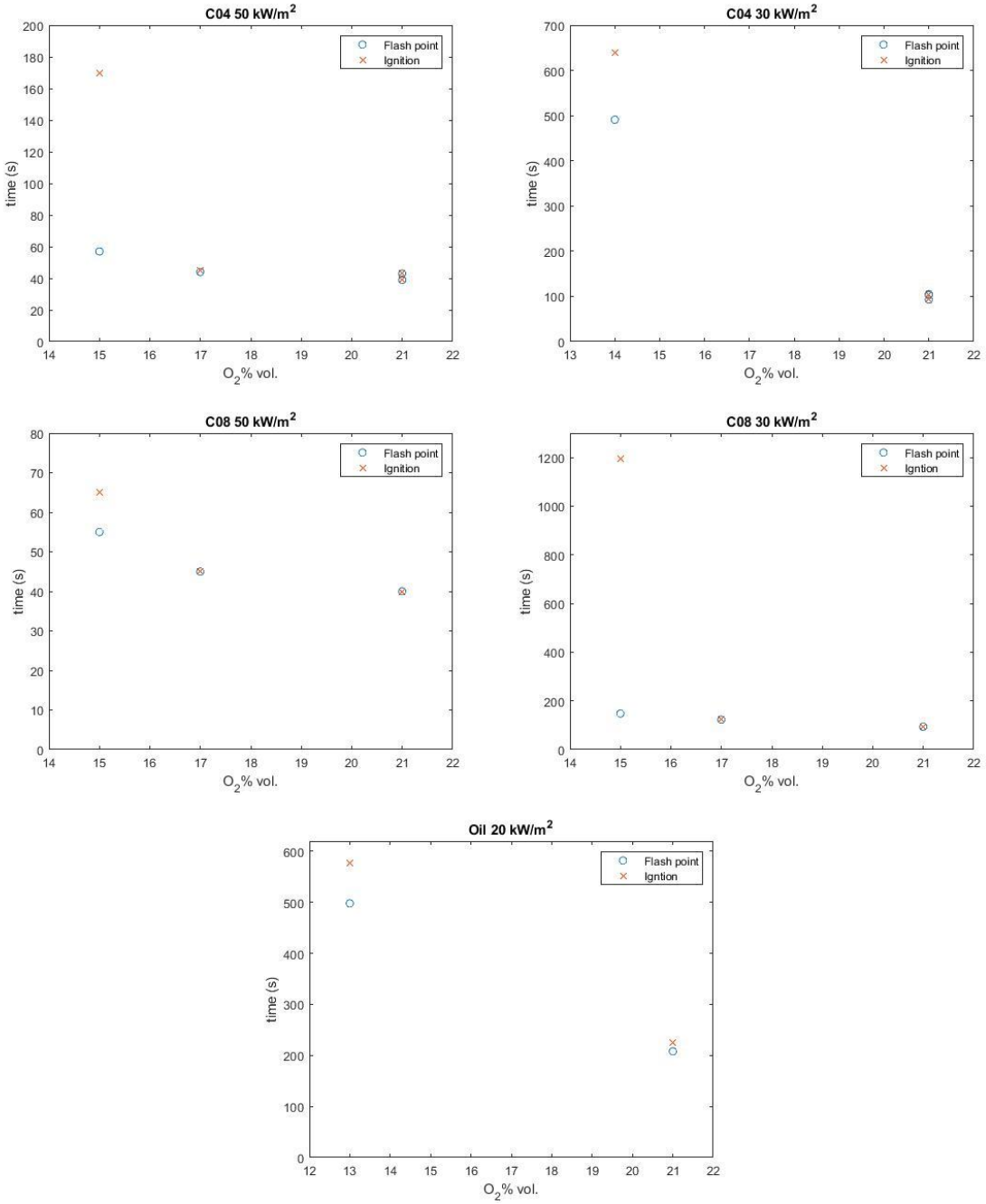

Figure 27 Flash point and ignition times for the oil, C04 and C08 at different O_2%

The ignition times increased for each fuel as the oxygen concentration decreased. For cable 4 and cable 8, the increase in ignition time was more substantial for the lower 30 kW/m^2 irradiance level than the 50 kW/m^2 irradiance level.

The time until the flash point stayed relatively constant for the cables. The exception was cable 4 at 30 kW/m^2. The time until the flash point increased substantially at an oxygen concentration of 14%. Cable 4 consists of different materials so it could be that the oxygen concentration was too low to ignite the outer part of the cable at 30 kW/m^2.

The increase in the time until the flash point for the oil is surprising though. It could be because the oxygen concentration is close to the limiting oxygen concentration or the flashing was missed because of the difficulty in seeing the surface of the oil. However, determining the reason for the increase in the time until flash point requires further investigation.

3.2 Heat release rate

A reduction in heat release rate has been observed for a variety of fuels when the oxygen concentration has been reduced below 21% using nitrogen as a diluent [9, 14, 19]. This can be attributed to a decrease in the flame temperature and a decrease in the emissivity of the flame caused by increased thermal capacity of the oxidizer due to a higher concentration nitrogen [14, 20].

There was generally a decrease in the HRRPUA when the oxygen concentration was reduced, but at an irradiance 50 kW/m^2 the reduction was less apparent for cable 4. This could be because the oxygen concentration reduces the heat release rate by reducing the heat transfer from the flame and not external radiant heat sources.

An exception to the decrease in the heat release rate is reported in Xin and Khan [21] were the peak heat release rate of PMMA at 15% O_2 and an applied irradiance of 30 kW/m^2 was the same as 21% O_2 for the same irradiance level. The peak heat release rate for both tests occurred at the end of the burning period, but the heat release rate for PMMA tested at 15% O_2 was below the test at 21% until the end of the burning period. This behavior was seen in cable 8 in both the HRRPUA and mass loss rate for an irradiance 50 kW/m^2 and a 17% O_2.

3.3 CO yield

Past studies have shown that the oxygen concentration affects the carbon monoxide yield. The carbon monoxide yield generally increased as the oxygen concentration was decreased below 21% [3, 4, 22, 23]. However, the CO yield did not always increase with decreasing oxygen concentration. In some cases, the carbon monoxide yield initially increased as the oxygen decreased, but as the oxygen concentration was decreased further the carbon monoxide yield also decreased [4, 22, 23].

In Figure 28, the carbon monoxide yields at different oxygen concentrations for the oil, cable 4 and cable 8 can be seen. The oxygen concentration didn’t seem to affect the carbon monoxide yield for the oil.

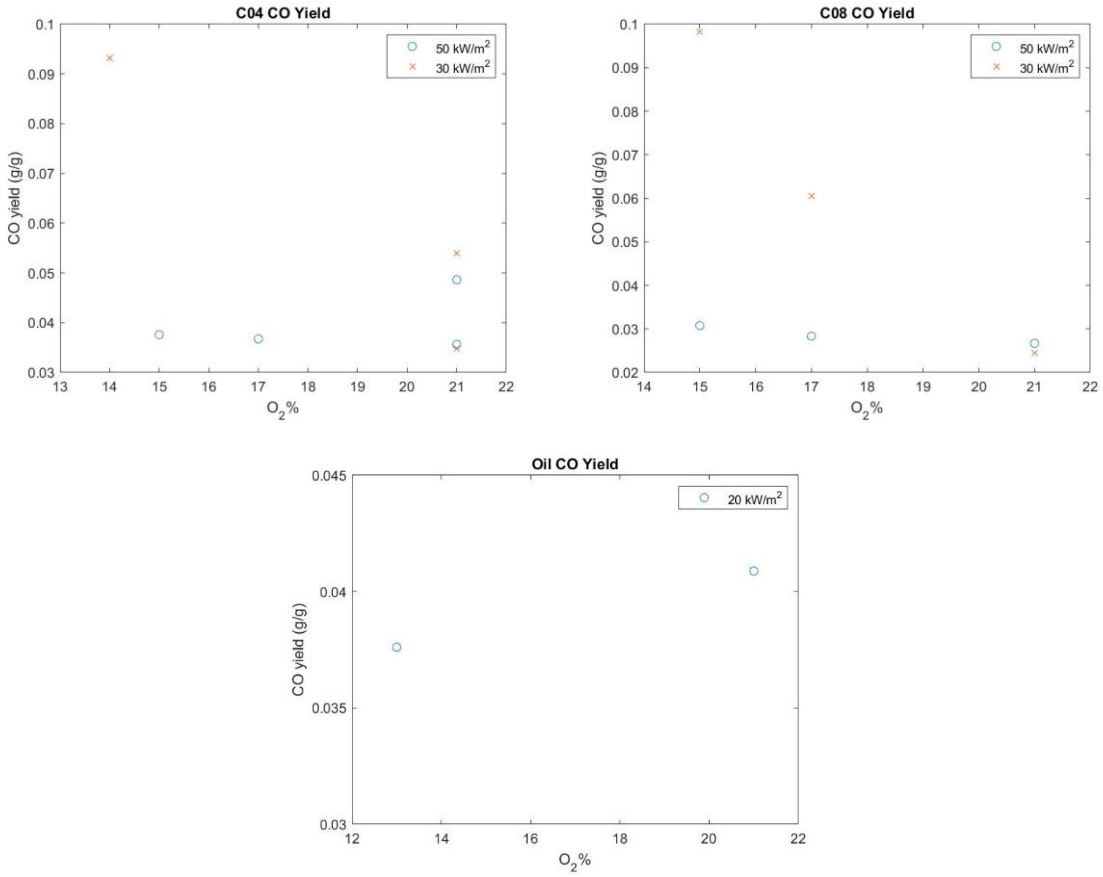

Figure 28 Carbon monoxide yields for the oil, C04 and C08 at different O_2%

The carbon monoxide yields for cables 4 and 8 stayed relatively constant at an irradiance of 50 kW/m^2. The carbon monoxide yield did increase for cables 4 and 8 at an irradiance 30 kW/m^2 when the oxygen concentration was lowered. However, this could be a result of partial burning over the surface area of the cables.

Partial burning over the surface area of the cables was observed during the tests with the increased carbon monoxide yields (T59, T60, and T67). For cable 4 at 14% O_2 and 30 kW/m^2 (T59), only one side of the exposed surface area of the cables was burning during the test. The carbon monoxide concentration measured by the analyzers in the duct before ignition was actually higher than during the burning period. For cable 8 at 17% O_2 and 30 kW/m^2 (T60), there was partial burning over the surface area during the beginning of the burning. At 15% O_2 and 30 kW/m^2 (T67), cable 8 burned only partially over the surface and very briefly.

4 Conclusion

- Tests at reduced oxygen concentrations were performed at irradiances of 20, 30, and 50 kW/m^2 for an oil, cable 4 (C04) and cable 8 (C08). At these conditions, the following conclusions can be made:
    - A reduction in the oxygen concentration generally resulted in a decrease in the mass loss rate and heat release rate per unit area (HRRPUA). However, cable 4 did not have a reduction in the mass loss rate and HRRPUA when exposed to an irradiance of 50 kW/m^2. Cable 8 also had a higher peak mass loss rate and peak HRRPUA when tested at an oxygen concentration of 17% though the mass loss rate and HRRPUA was lower than the standard cone calorimeter result for most of the test.
    - An increase in the ignition time when compared to tests done in the standard cone calorimeter occurred for the oil and both cables at the lowest oxygen concentration tested for each irradiance level.
    - The average carbon monoxide yields remained relatively constant or increased with decreases in the oxygen concentration.
    - The increase in carbon monoxide yield due to the decrease of oxygen concentration could be due lack of burning over the entire exposed surface area of the cables.
- The limiting oxygen concentration using nitrogen to dilute compressed air was also estimated at an irradiance of 20 kW/m^2 for the oil and 30 kW/m^2 for the cables. The estimated limiting oxygen concentrations were:
    - Oil: between 11% (no ignition) and 13% (ignition) at an irradiance of 20 kW/m^2
    - Cable 4: between 12% (no ignition) and 14% (ignition) at an irradiance of 30 kW/m^2
    - Cable 8: between 13% (no ignition) and 15% (ignition) at an irradiance of 30 kW/m^2

5 References

1. Peatross, M.J. and C.L. Beyler, *Ventilation effects on compartment fire characterization.* Fire Safety Science, 1997. **5**: p. 403-414.
2. Ingason, H., Y.Z. Li, and A. Lönnermark, *Fuel and Ventilation Controlled Fires*, in *Tunnel Fire Dynamics*. 2015, Springer New York: New York, NY. p. 23-43.
3. Mulholland, G., et al., *The effect of oxygen concentration on CO and smoke produced by flames.* Fire Safety Science, 1991. **3**: p. 585-594.
4. Brohez, S., G. Marlair, and C. Delvosalle, *The effect of oxygen concentration on CO and soot yields in fires.* Fire and Materials, 2008. **32**(3): p. 141-158.
5. Beyler, C., *Flammability Limits of Premixed and Diffusion Flames*, in *SFPE Handbook of Fire Protection Engineering*, M.J. Hurley, et al., Editors. 2016, Springer New York: New York, NY. p. 529-553.
6. Gottuk, D.T. and B.Y. Lattimer, *Effect of Combustion Conditions on Species Production*, in *SFPE Handbook of Fire Protection Engineering*, M.J. Hurley, et al., Editors. 2016, Springer New York: New York, NY. p. 486-528.
7. NIST. *Cone Calorimeter*. [cited 2017 December 1]; Available from: https://www.nist.gov/laboratories/tools-instruments/cone-calorimeter.
8. Technology, F.T. *Controlled Atmosphere Attachment*. [cited 2019 April 18]; Available from: http://www.fire-testing.com/Controlled-atmosphere-attachment.
9. Werrel, M., et al., *The calculation of the heat release rate by oxygen consumption in a controlled-atmosphere cone calorimeter.* Fire and Materials, 2014. **38**(2): p. 204-226.
10. STANDARDIZATION, E.C.F., *Plastics – Simple heat release test using a conical radiant heater and a thermopile detector (ISO 13927:2015)*. 2015, EUROPEAN COMMITTEE FOR STANDARDIZATION.
11. International Organization for Standardization, *ISO 5660-1:2015 Reaction-to-fire tests - Heat release, smoke production and mass loss rate* 2015.
12. Janssens, M., *Calorimetry*, in *SFPE Handbook of Fire Protection Engineering*, M.J. Hurley, et al., Editors. 2016, Springer New York: New York, NY. p. 905-951.
13. Drysdale, D., *Fire Science and Combustion*, in *An Introduction to Fire Dynamics*. 2011. p. 1-34.
14. Nilsson, M. and P. van Hees, *Advantages and challenges with using hypoxic air venting as fire protection.* Fire and Materials, 2014. **38**(5): p. 559-575.
15. Rich, D., et al., *Mass flux of combustible solids at piloted ignition.* Proceedings of the Combustion Institute, 2007. **31**(2): p. 2653-2660.
16. Rasbash, D.J., D.D. Drysdale, and D. Deepak, *Critical heat and mass transfer at pilot ignition and extinction of a material.* Fire Safety Journal, 1986. **10**(1): p. 1-10.
17. Cordova, J.L., et al., *Oxidizer Flow Effects on the Flammability of Solid Combustibles.* Combustion Science and Technology, 2001. **164**(1): p. 253-278.
18. Torero, J., *Flaming ignition of solid fuels*, in *SFPE Handbook of Fire Protection Engineering*. 2016, Springer New York. p. 633-661.
19. Marquis, D., E. Guillaume, and A. Camillo, *Effects of oxygen availability on the combustion behaviour of materials in a controlled atmosphere cone calorimeter.* Fire Safety Science, 2014. **11**: p. 138-151.
20. Beaulieu, P.A. and N.A. Dembsey, *Effect of oxygen on flame heat flux in horizontal and vertical orientations.* Fire Safety Journal, 2008. **43**(6): p. 410-428.
21. Xin, Y. and M.M. Khan, *Flammability of combustible materials in reduced oxygen environment.* Fire Safety Journal, 2007. **42**(8): p. 536-547.

22. Dowling, V.P., J. Leonard, and P. Bowditch, *Use of a controlled atmosphere cone calorimeter to assess building materials.* Proceeding in the 8th International Conference Fire science, 1999: p. 989-997.
23. Marsh, N.D. and R.G. Gann, *Smoke component yields from Bench-scale Fire Tests: 3. ISO 5660-1 / ASTM E 1354 with Enclosure and Variable Oxygen Concentration.* NIST Technical note, 2013. **1762**: p. 1-43.